C-Terminal Secretion Signal of an *Erwinia chrysanthemi* Protease Secreted by a Signal Peptide-Independent Pathway: Proton NMR and CD Conformational Studies in Membrane-Mimetic Environments†

Nicolas Wolff,‡ Jean-Marc Ghigo,§ Philippe Delepelaire,§ Cécile Wandersman,§ and Muriel Delepierre*,‡

Laboratoire de Résonance Magnétique Nucléaire, CNRS URA 1129, and Unité de Génétique Moléculaire, CNRS URA 1149, Institut Pasteur, 28 rue du Dr Roux, 75724 Paris Cedex 15, France

Received February 8, 1994; Revised Manuscript Received March 31, 1994®

ABSTRACT: The detailed structure of a 68-residue chimeric peptide encompassing the 56 last C-terminal residues of *Erwinia chrysanthemi* protease G has been investigated by using circular dichroism and NMR spectroscopies. The peptide which contains the secretion signal of PrtG was solubilized either in aqueous solvent, in trifluoroethanol (TFE)/H_2O mixtures, or in dodecyl β-D-maltoside detergent. The peptide helical content increases upon TFE and detergent additions. A stable conformation is reached at 40% TFE (v:v) and at a micelle to peptide ratio higher than 1. The ^1H NMR spectrum has been assigned in TFE/H_2O, 2:1 (v:v), and it is shown that residues 26–29 and 50–62 form a relatively stable helix although a conformational equilibrium between a helix and probably a more random structure is observed throughout fragment 13–63. Comparison of the CterG conformation with results obtained by deletion approach could lead to the hypothesis that the C-terminal secretion signal is composed of an α-helix located close to the essential C-terminal tetrapeptide D_{65}VIV.

In Gram-negative bacteria, whose envelope is made of two distinct membranes, a large majority of extracellular proteins is secreted by the signal peptide-dependent general secretory pathway (GSP) (Pugsley, 1993). The signal peptide located at the N-terminus of the secreted protein is engaged in the initial steps of targeting to and crossing of the cytoplasmic membrane, which involves the sec gene products. After cleavage of the signal peptide on the periplasmic side of the inner membrane (Gierasch, 1989), the protein released in the periplasmic space is transported across the outer membrane by a set of functions specific for each secreted protein by a yet unknown mechanism.

A second group of extracellular proteins without N-terminal cleavable signal peptide is secreted by a distinct secretion pathway (Holland *et al.*, 1990). In most cases, the secretion signal is located at the C-terminus of the secreted protein. Three specific membrane proteins constitute the secretion machinery: two located in the inner membrane, and one in the outer membrane. One of the inner membrane proteins belongs to the ATP binding cassette (ABC) family of proteins (Higgins, 1992). The secreted proteins cross both membranes without periplasmic intermediates, and their C-terminal signals are not cleaved during the membrane crossing. Mainly two families of protein are secreted via this signal peptide-independent pathway: a family of bacterial toxins such as *Escherichia coli* α-hemolysin (HlyA), *Pasteurella haemolytica* leukotoxin (LktA), and adenylate cyclase (CyaA) of *Bordetella pertussis*, and a family of metalloproteases such as those of *Erwinia chrysanthemi*, *Serratia marcescens* (PrtSM), and *Pseudomonas aeruginosa* (AprA). Today other types of protein have been identified that also use this secretion pathway (Wandersman, 1992). While within each family the proteins are highly homologous, this is not the case between proteins of different families. However, the homology is sufficient to allow exchange inside specific secretion systems as shown by functional complementation experiments in some cases (Létoffé *et al.*, 1990). Within the toxin family, the secretion of the *Escherichia coli* α-hemolysin is certainly the most studied, and there is still no agreement on the nature of the secretion signal. On the basis of secondary structure prediction and mutational analyses, it has been suggested that the C-terminal part of α-hemolysin is organized in three structural regions (Stanley *et al.*, 1991) or that only a few critical individual residues dispersed throughout the signal could act cooperatively during the secretion process (Kenny *et al.*, 1992).

The *E. chrysanthemi* protease family comprises four highly homologous metalloproteases PrtA, -B, -C, and -G (60% identity) (Delepelaire & Wandersman, 1990; Ghigo & Wandersman, 1992a,b). These four metalloproteases possess a C-terminal secretion signal and use the same secretion apparatus composed of three membrane proteins (PrtD, the ABC component, and PrtE in the cytoplasmic membrane and PrtF in the outer membrane) (Létoffé *et al.*, 1990; Delepelaire & Wandersman, 1991). This secretion signal can be fused to passenger proteins and promote in some cases their secretion in a PrtD/E/F-dependent fashion (Létoffé and Wandersman, 1992). The overall similarity of the 56 last residues in the *E. chrysanthemi* proteases is around 35%. It has been proposed that a putative amphipathic α-helix located in the 20 last residues could play a role in the secretion (Ghigo & Wandersman, 1992a). The secretion signal of the PrtG protease has been studied in greater detail, and it has been shown that the smallest autonomous secretion signal is made up of the 29 last residues of PrtG, although the secreted amount is substantially lower than that of a longer peptide containing the 56 last C-terminal residues (Ghigo & Wandersman, 1994). These results have also shown that the 15 last residues, when fused to a C-terminal truncated form of PrtG (not secreted),

† The work was supported by funds from the Institut Pasteur and the Centre National de la Recherche Scientifique.

* To whom correspondence should be addressed. Please send electronic mail to Murield@pasteur.fr.

‡ Laboratoire de Résonance Magnétique Nucléaire, CNRS URA 1129.

§ Unité de Génétique Moléculaire, CNRS URA 1149.

® Abstract published in *Advance ACS Abstracts,* May 15, 1994.

0006-2960/94/0433-6792$04.50/0

can still promote its secretion at a significant level and have also emphasized a potential role for the 4 last C-terminal residues in the secretion process.

The fact that N-terminal signal sequences have little conservation and that they are still functional when transferred from one protein to another has induced numerous structural studies on isolated signal peptides in various environments. It is known that they are generally poorly structured in aqueous environments while an α-helical structure of the hydrophobic core of the signal peptide is induced in nonpolar solvent, upon interaction with SDS[1] micelles or with phospholipid vesicles (Gierasch, 1989; Rizo *et al.*, 1993; Keller *et al.*, 1992).

However, no structural data are available yet on a C-terminal secretion peptide. Thus, in order to gain some insight into the secretion mechanism, we have studied in the present work the structure of PrtG C-terminal peptide (CterG) encompassing the secretion signal. This chimeric peptide, which contains the first 12 residues of β-galactosidase fused to the 56 last residues of PrtG, was chosen for its ease of purification from the culture supernatant, and its sequence is as follows: MTMITNSSSVPG-DLRFVDNFSGKGNEV-V L N W D S Q S H Q T N M W L H L S G H E T A D-FLVNIVGAALQPSDVIV (a hyphen has been inserted to indicate where residues derived β-galactosidase end and those from PrtG begin). There is no evidence of direct interaction between the C-terminal sequence and membrane lipids. However, the C-terminal peptide, like the whole protease, has to reach the membrane interface and to cross both membranes. Thus, the detailed structure of the C-terminal peptide has been determined using circular dichroism and NMR spectroscopies, in a membrane-like environment that is in apolar solvent such as trifluoroethanol. The results obtained are then compared with those obtained in H_2O and in interaction with micelles of dodecyl β-D-maltoside. The CterG is slightly soluble in aqueous solutions, but its solubility increases upon trifluoroethanol (TFE) or detergent addition together with its α-helical content. The structural results obtained here for the first time on a C-terminal secretion signal are discussed in relation with those obtained by a deletion approach on the secretion efficiency of various CterG derivatives.

MATERIALS AND METHODS

Purification. CterG was purified from 1 L of late-exponential phase culture supernatant of *E. coli* pop3 (pRUW4*inh*1, pRUW2005) grown at 30 °C in LB medium. PRUW4*inh*1 and pRUW2005 are two compatible plasmids expressing on one hand the secretion functions PrtD, PrtE, and PrtF (pRUW4*inh*1) and on the other hand the CterG peptide under the control of lac promoter (pRUW2005) (Ghigo & Wandersman, in press). After ammonium sulfate precipitation of the culture supernatant (45% saturation for 1 h at 4 °C), the pellet was resuspended in a minimal volume of 10 mM Tris-HCl, pH 8.0, 1 mM EDTA and dialyzed against the same buffer. After adjusting the dialysate with urea to 6 M, it was loaded on a Sephacryl S-200 HR column (55 × 1.5 cm, 90 mL) equilibrated with 10 mM Tris-HCl, pH 8.0, 150 mM NaCl, and 6 M urea. The CterG fractions were pooled and dialyzed against the same buffer without urea at a protein concentration of 1 mg/mL estimated by the OD_{280} measurement. The sample was then loaded onto a DE-52-cellulose column equilibrated with 10 mM Tris-HCl, pH 8.0, 150 mM NaCl, and 1 mM EDTA. At this salt concentration, CterG does not adsorb on the column, and the fractions were concentrated by precipitation with 45% saturated ammonium sulfate and dialyzed extensively against 10 mM phosphate buffer, pH 7.0, in a minimal volume. All the purification was performed at 4 °C. At every stage of purification, the sample was analyzed by SDS–polyacrylamide gel electrophoresis and Coomassie blue staining to estimate the protein purity (Figure 1). Finally, an amino acid analysis was performed to confirm the high level of purity and to have an estimation of the molar absorptivity (ϵ = 15 000 $M^{-1}\cdot cm^{-1}$). The yield was usually between 20 and 30 mg of purified CterG/L of culture. At the high concentrations required for the NMR studies, CterG has a high tendency to form a gel in aqueous solution. This tendency is increased at lower pH, higher temperature and higher salt concentration. These drawbacks were mostly circumvented by the use of detergent or TFE.

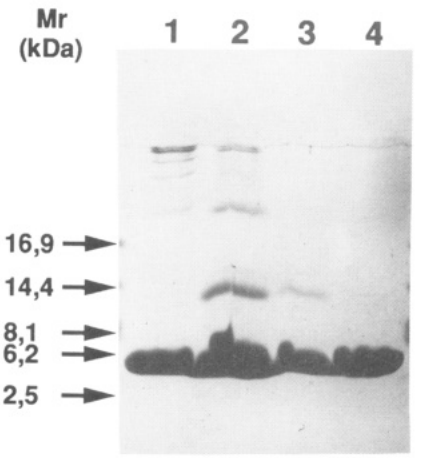

FIGURE 1: Coomassie blue staining after Tricine–SDS–PAGE analysis of CterG at each step of the purification on a 20% acrylamide gel. Lane 1: Culture supernatant after 20% TCA precipitation; lane 2: culture supernatant after 45% ammonium sulfate precipitation; lane 3: pooled fractions from gel filtration; lane 4: pooled fractions from DEAE chromatography. In each lane roughly 50 μg of protein was loaded.

Circular Dichroism. All CD measurements were made on a Jobin Yvon CD6 dichrograph at 25 °C with a 0.2-mm path length cylindric cell (Hellman). The ellipticity was calibrated with an aqueous solution of *d*-(+)-10-camphorsulfonic acid (Dorman & Maestre, 1973). Each spectrum was the average of three consecutive scans from 180 to 260 nm with 2 s of integration time/nm. The peptide concentration was 0.23 mg/mL (31 μM) as determined by quantitative amino acid analysis. TFE (Sigma) and phosphate buffer (10 mM, pH 7.0) were added to the peptide stock solution such that the final 16 TFE/phosphate buffer concentrations varied from 0% to 95% in TFE (v:v). Similarly, the detergent concentration varied from 34 μM to 23 mM (dodecyl β-D-maltoside was purchased from Calbiochem). The peptide concentration dependence of the ellipticities was measured over a peptide concentration range from 0.038 to 1.51 mg/mL (5.1 μM–0.205 mM) in a TFE/phosphate buffer, 2:1 (v:v), solution. Ellipticity is reported as mean residue molar ellipticity $[\theta]$, with the units of $deg\cdot cm^2\cdot dmol^{-1}$. The helical content was estimated using CD signal intensity according to the method of Chen *et al.* (1974). The CterG mean residue ellipticity at 220 nm, $[\theta]_{220}$, was compared to the theoretical mean residue ellipticity at 220 nm for a 68-residue peptide in 100% helical conformation, $[\theta]_{220}^{max}$ (Chen *et al.*, 1974; Scholtz *et al.*, 1991):

[1] Abbreviations: CD, circular dichroism; CMC, critical micellar concentration; COSY, correlated spectroscopy; EDTA, ethylenediaminetetraacetic acid; FID, free induction decay; NMR, nuclear magnetic resonance; NOE, nuclear Overhauser effect; RMS, root mean square; SDS, sodium dodecyl sulfate.

$$[\theta]_{220}^{max} = 40000(1 - k/n)$$

where k is a wavelength-dependent constant (2.60 at 220 nm) and n is the number of peptide residues. The calculated mean residue ellipticity at 220, $[\theta]_{220}^{max}$, is 38 500. Other values for infinite helix were also used (Yang *et al.*, 1986) instead of the 40 000 value leading to a 10% variation in the CterG α-helix content, which is smaller than the experimental errors.

Proton NMR Experiments. NMR spectra were recorded on a Varian Unity 500 spectrometer operating at 500 MHz for protons and equipped with Sun Sparc computers. Most spectra were recorded at 30 °C on samples containing 0.6–1 mM peptide dissolved in TFE-d_2-*OH*/H_2O, 2:1 (v:v) or in TFE-d_3/D_2O, 2:1 (v:v). TFE-d_2-*OH* and TFE-d_3 were 99% deuterium-enriched while D_2O was 99.9% deuterium-enriched (Euriso-top). The final salt concentration was 3 mM potassium phosphate, and the apparent pH was 7.0. The spectra are referenced to the central component of the multiplet due to the methylene resonance of TFE centered at 3.88 ppm downfield from external tetramethylsilane (TMS). Saturation of the solvent proton resonance was accomplished by selective irradiation during the relaxation time (1.5 s). In addition, for NOESY experiments (Kumar *et al.*, 1980), the solvent signal was saturated during the mixing time. In order to reduce the residual transversal magnetization, a homospoil pulse was applied at the beginning of both the relaxation delay and the mixing time in the NOESY pulse sequences. All the 2D experiments were collected using the States–Haberkorn method to produce phase-sensitive spectra (States *et al.*, 1982). In general, spectra were recorded with a sweep width of 5600 Hz in both dimensions and with 48 or 64 scans per t_1 increment. A total of 400, 512, or 600 FIDs of 2K complex data points were collected in t_2. For apodization, all the data were multiplied by a squared sine bell, shifted depending on the experiment, and zero filled to give a 4096 × 2048 data points matrix, respectively, in t_2 and t_1 prior to Fourier transformation. The through-bond proton resonance assignments were obtained in deuteriated and protonated solvents using the following sequences: purged COSY (P-COSY), double-quantum filtered COSY (DQF-COSY), double-quantum correlated spectroscopy (DQ), total correlated spectroscopy (clean TOCSY), while through-space sequential assignments as well as NOE patterns were deduced from nuclear Overhauser spectroscopy (NOESY). The P-COSY experiment (Marion & Bax, 1988) has quality comparable to that of the DQF-COSY experiment but has twice its sensitivity. However, the DQF-COSY (Piantini *et al.*, 1982; Rance *et al.*, 1983) was used for its smaller intensity of diagonal peaks. With the absence of diagonal peaks, the DQ (Boyd *et al.*, 1983) has been found to be particularly useful for the identification of strongly coupled peaks such as glycine αH protons. TOCSY experiments (Griesinger *et al.*, 1988) were recorded with mixing times of 50 and 80 ms using a coherence mixing obtained with the MLEV-17 pulse sequence. To avoid zero-quantum coherences particularly embarrassing at short mixing times, a 2% random variation in NOESY mixing time or a modified NOESY sequence was used (Sodano *et al.*, in preparation). In this new sequence, a 180° pulse was added in the mixing period with a varied position from scan to scan. NOE building curves were performed with 30 different peaks using NOESY experiments with mixing times of 60, 120, 180, and 200 ms. Spin diffusion effects were detected for mixing times greater than 120 ms.

Secondary Structure Predictions. The methods of Chou and Fasman (1979), Garnier *et al.* (1978), and Eisenberg *et al.* (1984) have been used for secondary structure predictions. These methods are included in the software packages GCG (Genetic Computer Group) and PCGENE (IntelliGenetics).

RESULTS

Circular Dichroism. The CD spectrum of CterG in aqueous solution (Figure 2a) is different from an unordered peptide spectrum (Chang *et al.*, 1978; Brahms & Brahms, 1980). However, it shows no clear characteristics of secondary structure. The TFE titration with the 16 points measured is shown in Figure 2a. From 0% to 15% TFE (v:v), the spectra show a maximum around 190 nm and a wide minimum around 212 nm. These extrema increase gradually upon TFE addition. The shape of these spectra could be significative of the presence of β-sheet structures (Chang *et al.*, 1978; Brahms & Brahms, 1980). In addition, an isodichroic point is observed at 202 nm, suggesting a two-state transition. Adding more TFE, from 20% (v:v) to 95%, induces a large change in the CD spectra, with a double minimum observed at 207 and 220 nm and a large maximum at 190–191 nm. These characteristics are indicative of an α-helix formation and show that the α-helical content of CterG is enhanced by increasing the TFE/H_2O ratio. Another isodichroic point is also observed at 201 nm from 20% to 95% TFE, suggesting a two-state conformational equilibrium, probably a helix–random coil interconversion. The ellipticity variation at 220 nm as a function of TFE concentration shows a double transition, approximately between 0% and 25% TFE (v:v) and between 70 and 95% TFE (v:v) (Figure 2b). The curve of the ellipticity at 207 nm as a function of TFE concentration is very similar to the curve at 220 nm, which displays a plateau between 40% and 70% TFE (v:v). An estimate of CterG helical content was obtained from the $[\theta]_{220}$ for TFE concentrations greater than 20%. Thus, estimation by fitting the experimental data to reference spectra either from Chang *et al.* (1978) or Brahms and Brahms (1980) gave high RMS. Several studies (Bruch *et al.*, 1989) have shown a good correlation between the estimates of helix content from experimental curve fitting and those from the simple method based on the $[\theta]_{220}$, even if there is an amount of β-strand (Walde *et al.*, 1993; Keller *et al.*, 1992). At concentrations corresponding to the plateau the α-helical content is estimated to be 60%, while at 95% TFE (v:v), the whole CterG peptide seems to be in α-helix conformation but immediately forms a gel at this concentration.

Similar spectral shape changes were observed upon dodecyl β-D-maltoside addition, a nonionic detergent (CMC: 0.17 mM; aggregation number: 98). Indeed, as illustrated in Figure 2c, below a detergent concentration corresponding to a 1:1 micelle to peptide ratio, the CD spectra display a maximum at 189 nm and a minimum at 211 nm which increase upon detergent addition. Like at 20% TFE (v:v), the spectrum shape, at a 1:1 micelle to peptide ratio, changes with a new minimum at 208 nm and with a shoulder around 220 nm, significative of α-helix formation. At higher detergent concentrations, the ellipticities at 208 and 220 nm remain constant, with superimposable spectra characteristic of α-helix (Figure 2c,d). From the $[\theta]_{220}$, the α-helix content at the plateau is estimated to be 47%.

Furthermore, at a fixed TFE/H_2O ratio of 2:1 (v:v) corresponding to the plateau, the CD spectra of CterG over a range of concentrations from 5 μM to 0.21 mM are invariant, suggesting either that CterG is monomeric or that aggregation of molecules is not detected by CD (data not shown).

NMR Experiments. The CterG peptide in aqueous buffer shows no clear evidence of a preferred secondary structure,

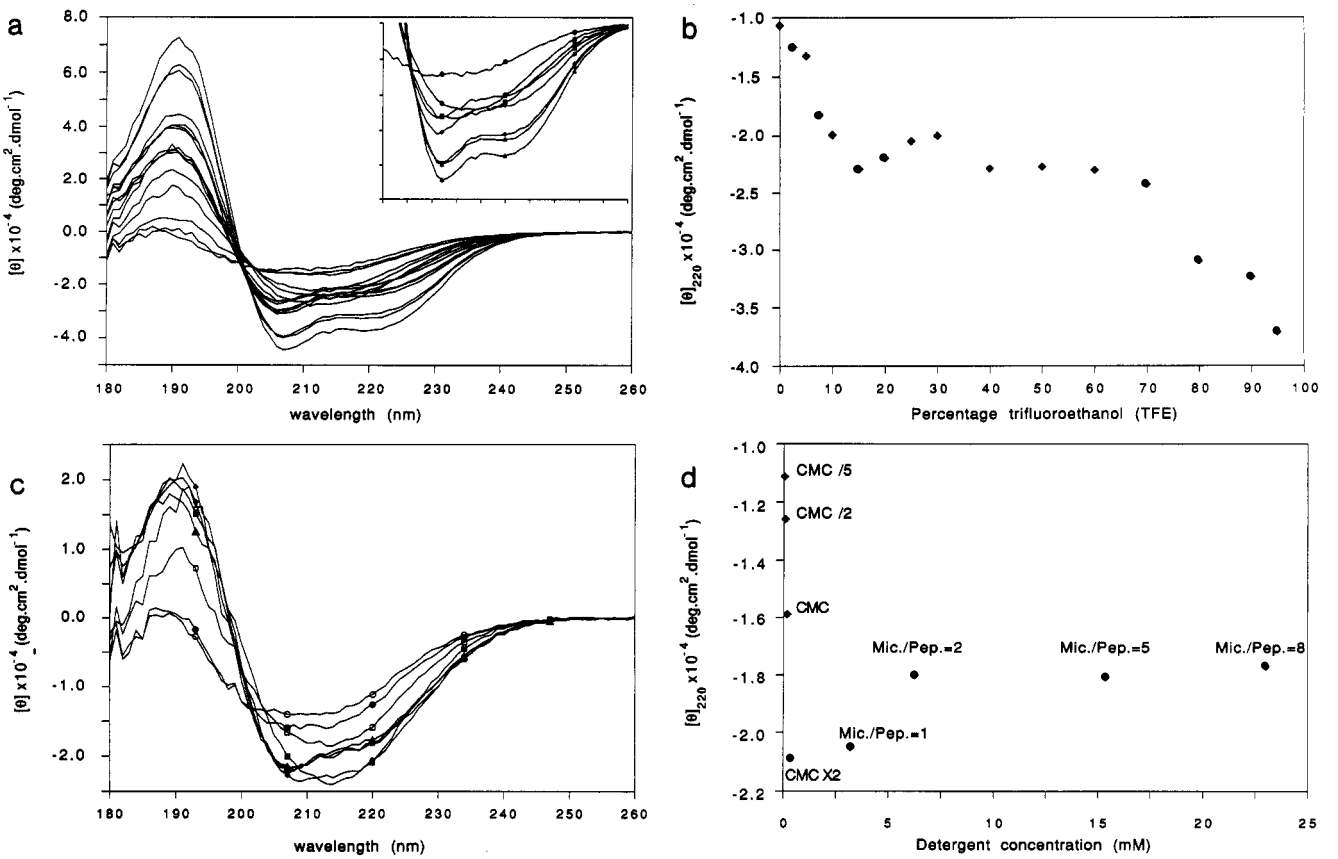

FIGURE 2: (a) CD spectra at 25 °C of CterG at 16 various concentrations of TFE and buffer (10 mM K_2HPO_4) pH 7.0. An extension between 195 and 245 nm for 8 TFE concentrations is represented in the upper right inset: (○): 0%; (●) 10%; (□) 20%; (■) 30%; (◊) 40%; (♦) 80%; (△) 90%; (▲) 95%. (b) Mean residue ellipticities at 220 nm, as a function of TFE concentration (v:v). (c) CD spectra at 25 °C of CterG at various concentrations of dodecyl β-D-maltoside/buffer (10 mM K_2HPO_4), pH 7.0: (○) CMC/5; (●) CMC/2; (□) CMC; (■) CMC × 2; (◊) mic./pep. = 1; (♦) mic./pep. = 2; (△) mic./pep. = 5; (▲) mic./pep.=8. (d) Mean residue ellipticities at 220 nm, as a function of dodecyl β-D-maltoside concentration (v:v).

in agreement with the CD results obtained in identical conditions. Indeed, lines are quite broad, and chemical shift dispersion is limited, rendering spin system identification very difficult, and thus no attempt in assigning resonances was done in aqueous solution. These observations combined with the results obtained by CD in the presence of TFE have driven us to choose a mixture of TFE and H_2O at a 2:1 ratio (v:v) for the structure determination by NMR. In spite of this, the peptide solution forms a gel 24 h after the peptide has been dissolved in the TFE/H_2O 2:1 (v:v), mixture. However, the absence of significant changes in line broadening as well as in peak intensity in 1D NMR spectra suggests that only a very small fraction of CterG molecules forms the gel. Nonetheless, a new sample was used for each 2D experiment to avoid modification in the 1D and 2D spectra. Of course, for samples arising from different purifications, the NMR spectra were carefully compared as far as line broadening, chemical shifts, and NOE patterns are concerned.

If the CD spectra can reveal global characteristics for the peptide secondary structures, the NMR spectra give local information on the residue conformation. Identification of the spin systems for each amino acid type (Wagner & Wüthrich, 1982; Redfield & Dobson, 1988) was achieved by means of through-bond connectivities using COSY-type experiments such as P-COSY (Figure 3), DQF-COSY, total correlation spectroscopy (TOCSY), and double-quantum correlated spectroscopy (DQ). This last experiment was very useful in identifying the degenerated chemical shifts of three glycine αH protons. The DQ spectra were also used to distinguish the βH of seven serines and the βH, δH for the Gln, Glu, and Met spin systems. This experiment was helpful

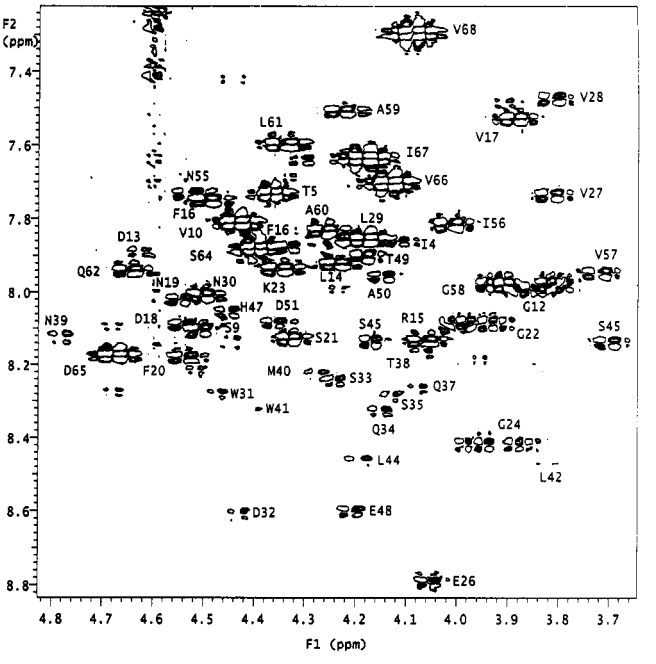

FIGURE 3: Fingerprint region of the phase-sensitive P-COSY spectrum of CterG at 30 °C in TFE/H_2O, 2:1 (v:v). The majority of backbone cross-peak assignments are indicated with a label. Both positive and negative contours are shown.

in the assignment process due to the absence of diagonal peaks, the spreading of peaks in one dimension, and the increase of peak number for each spin system since remote connectivities can be observed. The major difficulties in peak assignments

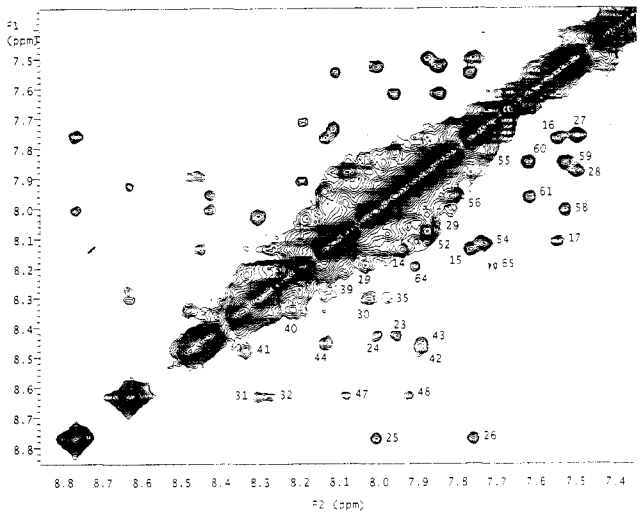

FIGURE 4: NH region of the phase-sensitive NOESY spectrum of CterG obtained at 30 °C in TFE/H_2O, 2:1 (v:v), with a mixing time of 120 ms. The majority of NH_i–NH_{i+1} cross-peak assignments are indicated with the NH_i label.

came from extensive overlaps of the βH protons of the AMX and AMPTX spin systems (27 residues) and the large number of methyl group, a total of 44. Furthermore, the peptide structure described below was not in favor of proton resonance dispersion. Finally, to unmask the proton peaks at resonances around 4.6 ppm in the αH–NH region, that is, close to the water frequency, the water peak was not irradiated on resonance but slightly downfield. A set of 2D experiments was performed in TFE-d_3/D_2O in order to discriminate between exchangeable and nonexchangeable protons such as the indole protons of the two Trp, the γNH_2 of five Asn, the δNH_2 of one Gln, and the ^2H, ^4H of the three His. In addition, the absence of solvent resonance increases the sensibility of the experiment and allowed us to observe the peaks around the water proton frequency. This has led to the identification of 64 spin systems.

Sequence-specific assignments were then determined from the cross-peaks in the 2D NOESY spectra recorded with 120- and 200-ms mixing times in which the NOE signals reflect the short distances between the αN, βN, and NN protons of adjacent amino acids (Figure 4). Knowing from CD that the molecule has a substantial helical content in this TFE to H_2O mixture, interactions between sequentially close residues are much more likely than interactions between residues which are far apart in the sequence. Thus, this assumption was used in sequential assignment and to complete the spin system attribution mainly from $\alpha\beta$ (i,i+3) and the NOEs between aromatic ring protons and surrounding residues (i,i+1; i,i+3). CterG contains 68 residues, of which 64 were identified; their proton chemical shifts are listed in Table 1. Among the four unidentified amino acids, three belong to the first twelve residues at the NH_2 extremity, that is, to the β-galactosidase. During the structure determination, this fragment of CterG was shown to adopt an extended chain conformation. The fourth missing residue is the Gly46, which might overlap with another glycine, but it was not possible to prove it. The presence of αH–δH (i,i+1) NOE for the two X-Pro dipeptide sequences is in favor of a high proportion of *trans* conformation. The pattern of interresidue NOEs obtained at 120-ms mixing time is displayed in Figure 5.

It has been shown previously by several groups (Pardi *et al.*, 1983; Wishart *et al.*, 1991) that the NH or αH protons chemical shifts are strongly dependent on the nature of protein secondary structure, with an upfield shift with respect to the random coil value being observed for residues in α-helices and a downfield shift for residues in β-strands. Two sets of chemical shifts for NH and αH in random coil were used (Bundi & Wüthrich, 1979; Wishart *et al.*, 1991). Although these values are extracted from tetrapeptides and protein data obtained in water, the random coil αH values are insensitive to the presence of TFE up to 30% (±0.02 ppm) (Jimenez *et al.*, 1987). At higher TFE concentrations, 40% (Sakai *et al.*, 1993) or 50% (Rizo *et al.*, 1993), the conformational shifts are in agreement with information on structural data obtained either from other NMR parameters or by CD. Figure 6 represents the NH and αH secondary shifts using the two above-mentioned sets of data. The majority of residues are located in the negative square. Thus, their αH and NH displayed upfield shifts, indicative of helix formation. The largest downfield shifts observed for αH concern, as expected, the residues preceding Pro11 and Pro63, while the largest downfield shifts observed for NH are those of the three aromatic amino acids Phe20, Trp31, and Trp41 and also the residues close enough to undergo the ring current effects (i,i+1; i,i+3; i,i+4). Complementary to this chemical shift analysis, Wishart *et al.* (1992) have proposed a fast and simple method to assess secondary structure solely based on the magnitude of these conformation-dependent secondary shifts, provided that a minimum number of adjacent residues (four for α-helices and three for β-strands) show induced shifts greater than 0.1 ppm. Using the rules defined by Wishart *et al.* (1992) and depending on the choice of reference values for proton chemical shifts in nonstructured peptides, two helices are found. Using random coil values (Wishart et al., 1992), the two helices extend from Pro11 to Ser21 and from Asn25 to Ala59. In addition, a small β-strand is predicted for residues 66–68 (Figure 7). Using, as proposed by Sakai *et al.* (1993) for studies in TFE, the coil values (Wishart *et al.*, 1991) that include all structures which are neither α-helix nor β-sheet, the two helices extend from residues 26 to 38 and from 40 to 57.

The identification of secondary structures was obtained through analysis of characteristic patterns of NOE cross-peaks (Figure 5). No long-range NOE indicative of tertiary structure has been identified. Cross-peaks indicative of helical structure were identified for a large fragment of the CterG sequence. Indeed, NN(i,i+1) connectivities of various intensity are observed all along the sequence between Leu14 and Val68 except around the glycine and proline residues and for the following fragments: Gln34–Gln37, Thr38–Asn39, and Leu53–Val54. The intensity of the αN(i,i) NOE cross-peak is greater than the intensity of the αN(i,i+1) cross-peak for most of the residues. Furthermore, the NN(i,i+1) cross-peaks are more generally intense than the αN(i,i+1) cross-peaks in the Leu14–Gln62 fragment. In the C-terminal region, fragment 63–68, the NN(i,i+1) cross-peaks are weaker, and only one medium-range NOE, $\alpha\beta$(i,i+3), is observed between residue Ala60 and Pro63. Contrastingly, in the central part of the peptide, from Asp13 to Pro63, a considerable number of $\alpha\beta$(i,i+3) NOE cross-peaks but only a few αN(i,i+3) and αN(i,i+4) NOEs can be detected. The lack of medium-range αN NOEs is explained in part by their weak expected intensities and the very important overlaps in the αN region of the 2D NOESY spectrum. Hence, it was very difficult to distinguish between absent and masked peaks. On the basis of the NOE pattern observed, that is, (i) the intensity of NN(i,i+1) cross-peaks, (ii) the low value for the αN(i,i+1)/αN(i,i) ratio, and (iii) the large number of medium-range NOEs $\alpha\beta$(i,i+3) and αN(i,i+3) between residues 13 and 63, it can be proposed that an α-helix is formed in this region.

Table 1: ^{1}H Chemical Shifts for PrtG's C-Terminal Peptide in TFE/H_2O[a]

residue	NH	αH–α′H	βH–β′H	γH–γ′H	δH–δ′H	others	
Met1	nd[b]	nd	nd	nd		nd	
Thr2	nd	3.60	4.13	1.24			
Met3	nd	4.53	2.06	2.56		nd	
Ile4	7.89	4.20	1.88	1.42	nd	nd	
Thr5	7.74	4.37	4.29	1.19			
Asn6	nd	nd	nd			nd	
Ser7	nd	4.45	3.96–3.87				
Ser8	nd	nd	nd				
Ser9	8.10	4.50	3.96–3.85				
Val10	7.82	4.44	2.11	0.97–0.93			
Pro11		4.33	2.23–1.93	2.05	3.85–3.61		
Gly12	7.99	3.91–3.86					
Asp13	7.90	4.63	2.89–2.67				
Leu14	7.93	4.25	1.67	1.71	0.93–0.87		
Arg15	8.14	4.08	1.74	1.67–1.61	3.18–3.06	NH	7.29–6.56
Phe16	7.76	4.51	3.28–3.09			2,6H	7.24
Val17	7.53	3.90	2.16	1.01–0.96			
Asp18	8.09	4.55	2.70				
Asn19	8.02	4.55	2.62			γNH_2	7.06–6.51
Phe20	8.19	4.53	3.21–3.03			2,6H	7.22
Ser21	8.13	4.34	3.98–3.95				
Gly22	8.09	4.01–3.93					
Lys23	7.94	4.36	1.90–1.81	1.44	1.68	ϵCH_2	2.98
Gly24	8.42	3.98–3.95					
Asn25	7.99	4.59	2.81			γNH_2	7.25–6.53
Glu26	8.80	4.07	2.11	2.36			
Val27	7.74	3.83	2.16	1.01–0.89			
Val28	7.48	3.83	2.15	1.01–0.88			
Leu29	7.86	4.24	1.74	1.58	1.00–0.89		
Asn30	8.01	4.53	2.89–2.83			γNH_2	7.42–6.66
Trp31	8.28	4.48	3.42			NH	9.53
						2H	7.22
						4H	7.60
						5H	7.09
						6H	7.15
						7H	7.38
Asp32	8.60	4.45	2.77–2.71				
Ser33	8.25	4.25	4.06–4.03				
Gln34	8.33	4.16	2.14	2.42–2.37		nd	
Ser35	8.29	4.14	3.83–3.69				
His36	7.96	4.45	3.23			2H	8.08
						4H	7.13
Gln37	8.26	4.08	2.18	2.44–2.35		nd	
Thr38	8.16	4.08	4.30	1.30			
Asn39	8.14	4.79	2.93–2.82			γNH_2	7.41–6.50
Met40	8.23	4.28	2.17	2.55–2.45		nd	
Trp41	8.33	4.41	3.51–3.41			NH	9.60
						2H	7.15
						4H	7.57
						5H	7.05
						6H	7.13
						7H	7.41
Leu42	8.48	3.83	1.89	1.43	0.89–0.83		
His43	7.90	4.42	3.31–3.23			2H	8.19
						4H	7.16
Leu44	8.47	4.20	1.82	1.57	0.89		
Ser45	8.14	4.18	3.69–3.42				
Gly46	nd	nd					
His47	8.05	4.45	3.24–3.15			2H	8.25
						4H	7.17
Glu48	8.60	4.21	2.09–2.06	2.32			
Thr49	7.91	4.20	4.30	1.27			
Ala50	7.96	4.16	1.44				
Asp51	8.09	4.37	2.70				
Phe52	7.89	4.34	3.28			2,6H	7.22
						3,5H	7.26
Leu53	8.11	4.01	1.86	1.58	0.92		
Val54	8.15	3.71	2.13	1.05–0.93			
Asn55	7.74	4.53	2.86–2.64			γNH_2	7.43–6.59
Ile56	7.82	4.02	1.89	1.42–1.17	0.75	γCH_3	0.81
Val57	7.95	3.73	2.18	0.93–0.81			
Gly58	7.99	3.93–3.86					
Ala59	7.51	4.24	1.45				
Ala60	7.84	4.27	1.46				
Leu61	7.60	4.35	1.73	1.60	0.90–0.85		
Gln62	7.95	4.66	2.02	2.43–2.17		δNH_2	6.43–7.42
Pro63		4.41	2.30–1.98	2.08	3.81–3.71		

Table 1 (Continued)

residue	NH	αH–α'H	βH–β'H	γH–γ'H	δH–δ'H	others	
Ser64	7.89	4.41	3.98–3.83				
Asp65	8.19	4.68	2.73				
Val66	7.71	4.15	2.12	0.92			
Ile67	7.65	4.20	1.86	1.51–1.18	0.90	γCH_3	0.87
Val68	7.31	4.10	2.07	0.89			

[a] All data were obtained in TFE-d_2-*OH*/H_2O or in TFE-*d*/D_2O, 2:1 (v:v). Chemical shifts are in ppm relative to the CH_2 of TFE (3.88 ppm downfield from TMS) and are accurate to ±0.02 ppm. Values are for PrtG's peptide at 30 °C, apparent pH 6.8, and peptide concentration 0.7–1.0 mM. [b] nd: chemical shift not determined.

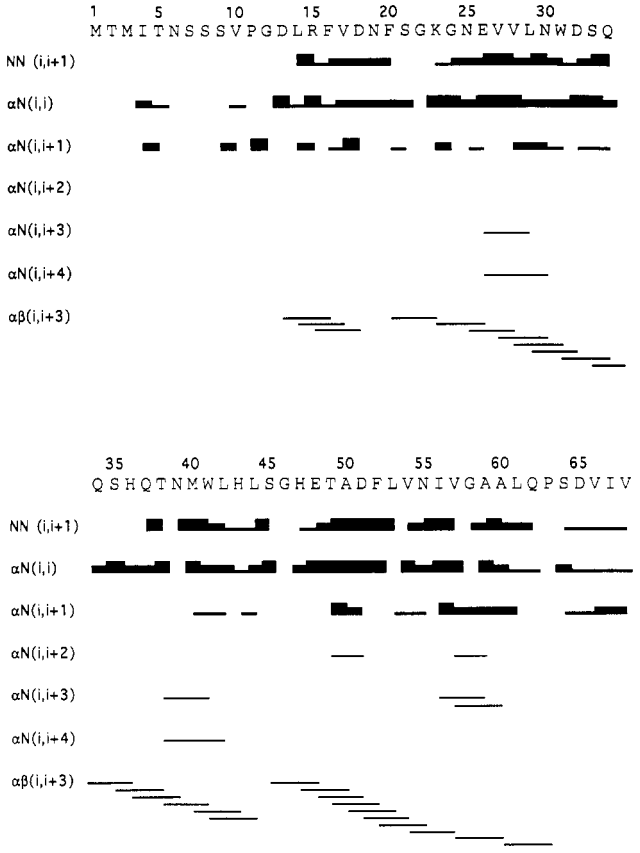

FIGURE 5: Summary of backbone NOE connectivities for CterG at 30 °C and at TFE/H_2O, 2:1 (v:v). The mixing time was 120 ms. NOE intensities are classified into three groups according to the volume of the cross-peaks. The thickness of the lines indicate the strong, medium, and weak NOE intensities.

Two $\alpha N(i,i+2)$ were also identified for Thr49–Asp51 and Val57–Ala59 characteristic of 3_{10}-helix. In the NH_2-terminal region, both the lack of assignment for 3 residues and the lack of medium-range NOEs between residues 1 and 12 argue strongly that this fragment adopts an extended chain conformation. There were not sufficient NMR data, mainly due to resonance overlap, to perform molecular modeling of the structure of the CterG peptide and particularly to delimit more precisely the boundaries of the helices.

We have shown that the CterG signal peptide from residues 13 to 63 adopts an α-helix conformation. However, differences in the medium-range NOE pattern are observed for the whole α-helical region. This feature probably results from an equilibrium between a helical and a more random structure, although other structural and/or relaxation effects could be involved in these NOE variations. However, from NMR and CD parameters, there is no evidence of the presence of other secondary structure. Nevertheless, the relative stability of the helical fragment was probed by measuring NH exchange rates of amide protons with D_2O. Unfortunately, the poor solubility of the peptide at acidic pH did not allow us to measure these rates. At 30 °C and pH 7, all amide protons had been exchanged with solvent deuterium in 20 min. To overcome this drawback, the relative helix stability was deduced from NOESY experiments run at 40 °C. Of course, as rightly pointed out by Bruch *et al.* (1989), there are several reasons why NOEs may be smaller at higher temperature such as changes in solution viscosity or in conformation or both. However, comparison of $NN(i,i+1)$ cross-peak intensities within the 40 °C NOESY map of different regions can still reflect differences in conformational stability. The pattern of NOEs observed at 40 °C (Figure 8) shows that the most stable helix is localized in the 50–62 fragment although few NH–NH interactions are maintained along the 26–29 fragment (Figure 8) as well as weak interactions for the 39–44 and 64–66 fragments. As a rule, the strongest NOEs observed at 30 °C are those which are maintained at 40 °C.

DISCUSSION

This paper describes the first CD and NMR conformational study of a peptide secreted independently of the general secretory pathway. This peptide (CterG) carries the C-terminal secretion signal of the *E. chrysanthemi* metalloprotease G. Whereas CterG shows no clear preference for a particular secondary structure in an aqueous environment, a helical conformation is observed in apolar environments. The CD shape changes upon detergent or TFE addition are very similar. Below 20% TFE (v:v) or a micelle to peptide ratio of 1, the CD curves could reflect a conformational transition involving β-sheet structure. The curve fitting did not allow us to estimate the β-sheet content. Moreover, it has not been possible to characterize this structure since at these low TFE concentrations the sample forms a gel instantaneously, preventing NMR analysis. For higher TFE and detergent concentrations, the CD spectra are characteristic of α-helix formation. The stabilizing effect of TFE was reached around 40%, implying that the inherent helical propensity of the CterG peptide is high (Nelson & Kallenbach, 1989; Lerhman *et al.*, 1990; Zhou *et al.*, 1990). In detergent the plateau is reached at a micelle to peptide ratio greater than 1, allowing the assumption that one molecule of CterG is interacting with a single micelle in an α-helix conformation. From CD measurements, estimation of a helical content by measuring the mean residue ellipticity at 220 nm was calculated only for spectra characteristic of α-helix, that is, at TFE concentrations greater than 40% or micelle to peptide ratios greater than 1. Thus 60% of α-helix content is obtained in TFE and 47% in micellar environments. Although the helical content in detergent is lower than in TFE solution, the agreement is still reasonable, allowing the assumption of a similar conformation in these two environments, as already observed in several studies of peptides (Mammi & Peggion, 1990; Macquaire *et al.*, 1993) and signal peptides (Yamamoto *et al.*, 1990; Rizo *et al.*, 1993). From NMR analysis of the CterG peptide, the more stable α-helices can be proposed for fragments 26–29 and 50–62, but with a conformational equilibrium between

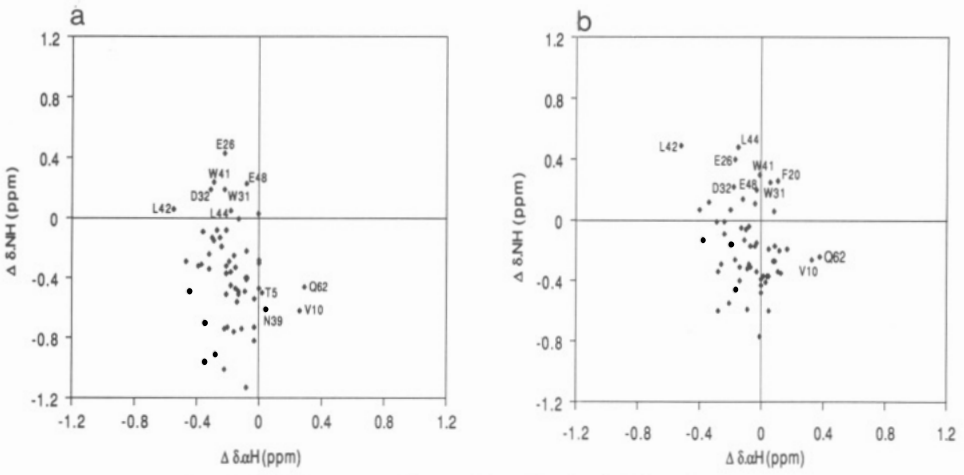

FIGURE 6: 2D plot of NH secondary chemical shifts versus αH secondary chemical shifts. The labels indicate the residues with highest positive NH or αH secondary chemical shifts. (a) From random coil values defined by Bundi and Wüthrich (1979). (b) From coil values defined by Wishart *et al.* (1991).

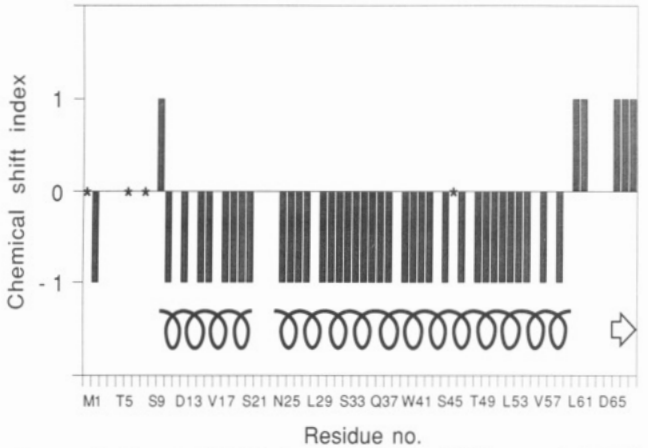

FIGURE 7: Chemical shift index described by Wishart *et al.* (1992) versus the CterG sequence. The CSI was calculated using the αH coil values given in Table 2 of Wishart *et al.* (1992). The helices and β-strand deduced from the CSI method are schematically shown. The asterisks indicate the residues for which there is no αH assignment.

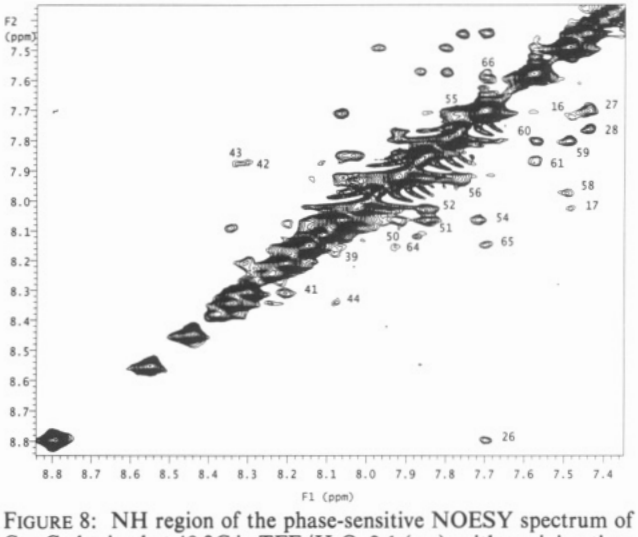

FIGURE 8: NH region of the phase-sensitive NOESY spectrum of CterG obtained at 40 °C in TFE/H_2O, 2:1 (v:v), with a mixing time of 100 ms. The majority of NH_i–NH_{i+1} cross-peak assignments are indicated with the NH_i label. The imperfections near the diagonal are due to the peptide instability during the experiment at this temperature.

an α-helix and other structures including random coil throughout fragment 13–63. The first 12 N-terminal residues, which belong to the β-galactosidase, do not show secondary

```
                15   20   25   30   35   40   45   50   55   60   65
CterA   NLHFV-N-QFSGSGGFILLNWDSSASVSNLYLNLDNNTSHEPQVKIVGQVSQTADFVV
CterB   QLSFVQ-DQFTGKGQEVMLQWDAANSTTNLWLHEAGHSSVDFLVRIVGQTAQ-SDIIV
CterC   QLSFVQ-DQFTGKGQEVMLQWDAANSITNLWLHEAGHSSVDFLVRIVGQAAQ-SDIIV
CterG   DLRFV--DNFSGKGNEVVLNWDSQSHQTNMWLHLSGHETADFLVNIVGAALQPSDVIV

AprA    VLQYV--DAFAGNAQGI-LSYDAASKAGSLAVDFSGDRHADFAINLIGQATQ-ADIVL
```

FIGURE 9: C-Terminal sequence alignment of the four *E. chrysanthemi* metalloproteases: CterA, CterB, CterC, and CterG. The residues strictly conserved are indicated in bold characters. The C-terminal of alkaline protease of *P. aeruginosa* AprA is represented too. The residues common with those of CterG are indicated in bold characters.

structure even in TFE. The sequence SSSVPG is unfavorable for the formation of an α-helix, showing that TFE itself does not induce, as expected, spurious helix formation (Nelson & Kallenbach, 1989; Lehrman *et al.*, 1990; Sönnichsen *et al.*, 1992).

Correlation between the ability to interact with phospholipid vesicles, the hydrophobicity, and their biological functions has been established for N-terminal signal peptides. Particularly, the hydrophobic core (McKnight *et al.*, 1989; Doud *et al.*, 1993), which is the main part of the helix, is probably inserted in the bilayer as shown for LamB (McKnight *et al.*, 1991) or OmpA (Rizo *et al.*, 1993). Indeed, if a hydrophobic region (Eisenberg, 1984) has been found between residues Phe52 and Leu61 of the CterG peptide, this is less obvious for the C-terminal region of the other proteases known as A, B, and C from *E. chrysanthemi* (Figure 9), although all of these use an identical export pathway. However, this region is predicted, for the four sequences, to be structured in amphiphilic helix (Eisenberg *et al.*, 1984) on the basis of the hydrophobic moment calculation. Sequence alignment of the four *E. chrysanthemi* metalloprotease C-terminal regions shows that among the 56 residues 19 are strictly conserved. The sequences contain 4–6 negatively charged amino acids against 1–2 positively charged ones.

The structure of the mature alkaline protease from *P. aeruginosa*, which can use *E. chrysanthemi* metalloprotease secretion functions (Guzzo *et al.*, 1991), has been determined at atomic resolution by XR diffraction studies (Baumann *et al.*, 1993). The XR structure reveals that the C-terminal domain of the protein is composed of only β-sheets and can bind weakly in its 50 last residues a calcium ion. If one assumes that the C-terminal part of this protease, which displays 32% identity with that of PrtG (Figure 9), can adopt an α-helix

conformation in the micelle environment, this points to the conformational interconvertibility of these extremities which might be related to the secretion process. The secondary structure predictions (Garnier *et al.*, 1978; Chou & Fasman, 1979) for CterA, -B, -C, and -G give a high content of β-strand, always higher than the α-helix content. For CterG, the presence of β-strand secondary structure is a possibility at low TFE and detergent concentrations or in water. However, at higher TFE concentrations or in the micelle environment, the α-helical structure is predominant. For the N signal peptides, Gierasch (1989) has pointed out the conformational interconvertibility depending on their environment and its probable biological implication (Briggs *et al.*, 1986; Reddy & Nagaraj, 1989).

These results together with those (Ghigo & Wandersman, 1994) obtained by a deletion approach either on CterG itself or on CterG fused at the C-terminus of a truncated and nonsecreted form of PrtG could potentially lead to a better understanding of the secretion process. In that respect the observation of the formation of an α-helix both in TFE and in a micelle environment suggests that such a structure could be formed during the secretion process. The deletion approach has identified an essential tetrapeptide motive found at the extreme C-terminus of CterG ($D_{65}VIV_{68}$), which was found to be unstructured. In the four metalloprotease C-terminal extremities, this motive is highly conserved. The most stable helix is found between residues 50 and 62, and it has been shown that this region is also essential to obtain a high level of secretion. However, another similar tetrapeptide motive is found at positions $D_{51}FLV_{54}$. Progressive deletions, removing either 4, 8, or 12 residues from the C-terminus, reduced the secretion efficiency to less than 0.1%. However, a 14-residue deletion bringing the secondary $D_{51}FLV$ motive at the extreme C-terminus restored the secretion to 50%. This secondary motive is part of one of the most stable α-helix, but it is possible that, when exposed at the C-terminus of the molecule, it does not adopt any longer a helical conformation, considering also the lower stability of the helix in the 40–50 region. However, in that case (i.e., $D_{51}FLV$ at the C-terminus of the protein), further deletion of the 12–31 region either on CterG or on the whole protease PrtG (J.-M. Ghigo, unpublished results) completely abolishes the secretion. This region is part of the other stable α-helix found in CterG. Thus, from these results, it is clear that although necessary this motive is not sufficient to promote the secretion and the region upstream also has a strong influence on the secretion efficiency. A working hypothesis would be that the secretion signal is composed at least of an α-helix located close to a tetrapeptide motive (DFLV/DVIV) at the C-terminus. Several models have been proposed on the hemolysin secretion with as yet no available structural data (Stanley *et al.*, 1991; Kenny *et al.*, 1992), and we hope that further structural studies of other C-terminal extremities could lead toward a common model of peptide interactions with the membrane environment and the transport system.

ACKNOWLEDGMENT

We thank Thierry Rose for advice in CD technique and interpretation as well as helpful discussions, and we appreciate the expert technical assistance of Catherine Simenel for NMR.

REFERENCES

Baumann, U., Wu, S., Flaherty, K. M., & McKay, D. B. (1993) *EMBO J. 12*, 3357–3364.
Boyd, J., Dobson, C. M., & Redfield, C. (1983) *J. Magn. Reson. 55*, 170–176.
Brahms, S., & Brahms, J. (1980) *J. Mol. Biol. 138*, 149–178.
Briggs, M. S., Cornell, D. G., Dluhy, R. M., & Gierasch, L. M. (1986) *Science 233*, 206–208.
Bruch, M. D., McKnight, C. J., & Gierasch, L. M. (1989) *Biochemistry 28*, 8554–8561.
Bundi, A., & Wüthrich, K. (1979) *Biopolymers 18*, 285–298.
Chang, C. T., Wu, C.-S. C., & Yang, J. T. (1978) *Anal. Biochem. 91*, 13–31.
Chen, Y.-H., Yang, J. T., & Chau, K. H. (1974) *Biochemistry 13*, 3350–3359.
Chou, P. Y., & Fasman, G. D. (1979) *Biophys. J. 26*, 367–384.
Delepelaire, P., & Wandersman, C. (1990) *J. Biol. Chem. 265*, 17118–17125.
Delepelaire, P., & Wandersman, C. (1991) *Mol. Microbiol. 5*, 2427–2434.
Dorman, H. J., & Maestre, M. F. (1973) *Proc. Natl. Acad. Sci. U.S.A. 70*, 255–259.
Doud, S. K., Chou, M. M., & Kendall, D. A. (1993) *Biochemistry 32*, 1251–1256.
Eisenberg, D. (1984) *Annu. Rev. Biochem. 53*, 595–623.
Eisenberg, D., Weiss, R. M., & Terwilliger, T. C. (1984) *Proc. Natl. Acad. Sci. U.S.A. 81*, 140–144.
Garnier, J., Osguthorpe, D. J., & Robson, B. (1978) *J. Mol. Biol. 120*, 97–120.
Ghigo, J.-M., & Wandersman, C. (1992a) *Res. Microbiol. 143*, 857–867.
Ghigo, J.-M., & Wandersman, C. (1992b) *Mol. Gen. Genet. 236*, 135–144.
Ghigo, J.-M., & Wandersman, C. (1994) *J. Biol. Chem. 269*, 8979–8985.
Gierasch, L. M. (1989) *Biochemistry 28*, 923–930.
Griesinger, C., Otting, G., Wüthrich, K., & Ernst, R. R. (1988) *J. Am. Chem. Soc. 110*, 7870–7872.
Guzzo, J., Duong, F., Wandersman, C., Murgier, M., & Lazdunski, A. (1991) *Mol. Microbiol. 5*, 447–453.
Higgins, C. F. (1992) *Annu. Rev. Cell. Biol. 8*, 67–113.
Holland, I. B., Blight, M. A., & Kenny, B. (1990) *J. Bioenerg. Biomembr.* 22, 473–491.
Jimenez, M. A., Nieto, J. L., Herranz, J., Rico, M., & Santoro, J. (1987) *FEBS Lett. 221*, 320–324.
Keller, R. C. A., Killian, J. A., & De Kruijff, B. (1992) *Biochemistry 31*, 1672–1677.
Kenny, B., Taylor, S., & Holland, I. B. (1992) *Mol. Microbiol. 6*, 1477–1489.
Kumar, A., Ernst, R. R., & Wüthrich, K. (1980) *Biochem. Biophys. Res. Commun. 95*, 1–6.
Lehrman, S. R., Tuls, J. L., & Lund, M. (1990) *Biochemistry 29*, 5590–5596.
Létoffé, S., & Wandersman, C. (1992) *J. Bacteriol. 174*, 4920–4927.
Létoffé, S., Delepelaire, P., & Wandersman, C. (1990) *EMBO J. 9*, 1375–1382.
Macquaire, F., Baleux, F., Huynh-Dinh, T., Rouge, D., Neumann, J.-M., & Sanson, A. (1993) *Biochemistry 32*, 7244–7254.
Mammi, S., & Peggion, E. (1990) *Biochemistry 29*, 5265–5269.
Marion, D., & Bax, A. (1988) *J. Magn. Reson. 80*, 528–533.
McKnight, C. J., Briggs, M. S.., & Gierasch, L. M. (1989) *J. Biol. Chem 264*, 17293–17297.
McKnight, C. J., Rafalski, M., & Gierasch, L. M. (1991) *Biochemistry 30*, 6241–6246.
Nelson, J. N., & Kallenbach, N. R. (1989) *Biochemistry 28*, 5256–5261.
Pardi, A., Wagner, G., & Wüthrich, K. (1983) *Eur. J. Biochem. 137*, 445–454.
Piantini, U., Sorensen, O. W., & Ernst, R. R. (1982) *J. Am. Chem. Soc. 104*, 6800–6801.
Pugsley, A. P. (1993) *Microbiol. Rev. 57*, 50–108.
Rance, M., Sorensen, O. W., Bodenhausen, G., Wagner, G., Ernst, R. R., & Wüthrich, K. (1983) *Biochem. Biophys. Res. Commun. 117*, 479–485.
Redfield, C., & Dobson, C. M. (1988) *Biochemistry 27*, 122–136.

Reddy, G. L., & Nagaraj, R. (1989) *J. Biol. Chem. 28*, 16591–16597.
Rizo, J., Blanco, F. J., Kobe, B., Bruch, M. D., & Gierasch, L. M. (1993) *Biochemistry 32*, 4881–4894.
Sakai, T. T., Jablonsky, M. J., DeMuth, P. A., & Krishna, N. R. (1993) *Biochemistry 32*, 5650–5655.
Scholtz, J. M., Qian, H., York, E. J., Steward, J. M., & Baldwin, R. L. (1991) *Biopolymers 31*, 1463–1470.
Sönnichsen, F. D., Van Eyk, J. E., Hodges, R. S., & Sykes, B. D. (1992) *Biochemistry 31*, 8790–8798.
Stanley, P., Koronakis, V., & Hughes, C. (1991) *Mol. Microbiol. 5*, 2391–2403.
States, D. J., Haberkorn, R. A., & Ruben, D. J. (1982) *J. Magn. Reson. 48*, 286–292.
Wagner, G., & Wüthrich, K. (1982) *J. Mol. Biol. 155*, 347–366.
Walde, P., Han, D., & Luisi, P. L. (1993) *Biochemistry 32*, 4029–4034.
Wandersman, C. (1992) *Trends Genet. 8*, 317–321.
Wishart, D. S., Sykes, B. D., & Richards, F. M. (1991) *J. Mol. Biol. 222*, 311–333.
Wishart, D. S., Sykes, B. D., & Richards, F. M. (1992) *Biochemistry 31*, 1647–1651.
Yamamoto, Y., Ohkubo, T., Kohara, A., Tanaka, T., & Kikuchi, M. (1990) *Biochemistry 29*, 8998–9006.
Yang, J. T., Wu, C.-S. C., & Martinez, H. M. (1986) *Methods Enzymol. 130*, 209–269.
Zhou, N. E., Mant, C. T., & Hodges, R. S. (1990) *Peptide Res. 3*, 8–20.